THE ASTROPHYSICAL JOURNAL, 565:1191–1204, 2002 February 1

MAGNETICALLY LINKED STAR-DISK SYSTEMS. I. FORCE-FREE MAGNETOSPHERES AND EFFECTS OF DISK RESISTIVITY

DMITRI A. UZDENSKY, ARIEH KÖNIGL,[1] AND C. LITWIN[2]
Department of Astronomy and Astrophysics, University of Chicago, 5640 South Ellis Avenue, Chicago, IL 60637;
uzdensky@oddjob.uchicago.edu, arieh@jets.uchicago.edu
Received 2000 November 13; accepted 2001 October 4

ABSTRACT

We consider the interaction between a magnetic star and its circumstellar disk under the assumption that the stellar magnetic field permeates the disk and that the system's magnetosphere is force-free. Using simplified axisymmetric models (both semianalytic and numerical), we study the time evolution of the magnetic field configuration induced by the relative rotation between the disk and the star. We show that if both the star and the magnetosphere are perfectly conducting, then there is a maximum disk surface conductivity $\Sigma_{\rm max}$ for which a steady state field configuration can be established. For larger values of conductivity, no steady state is possible, and the field lines inflate and effectively open up when a critical twist angle (which for an initially dipolar field is on the order of a few radian) is attained. We argue that for thin astrophysical disks, surface conductivities are likely to exceed the local $\Sigma_{\rm max}$ except in the immediate vicinity of the corotation radius in a Keplerian disk. If the disk conductivity is high enough, then the radial magnetic field at the disk surface will become large and induce radial migration of the field lines across the disk. We find, however, that the radial diffusion in the disk is generally much slower than the field-line expansion in the magnetosphere, which suggests that the opening of the magnetosphere is achieved before the diffusive outward expulsion of the field lines from the disk can occur. The effects of magnetospheric inertial effects and of field-line reconnection are considered in the companion paper.

Subject headings: accretion, accretion disks — MHD — stars: formation — stars: magnetic fields — stars: pre–main-sequence — stars: winds, outflows

1. INTRODUCTION

Disk accretion onto a magnetic star is thought to have important observational consequences for neutron stars, white dwarfs, and young stellar objects (YSOs). In particular, if the stellar magnetic field penetrates the disk, it may transmit torques between the disk and the star, providing a possible explanation for the spin-up/spin-down episodes in X-ray pulsars (e.g., Ghosh & Lamb 1978, 1979a, 1979b, hereafter GL; Wang 1987; Lovelace, Romanova, & Bisnovatyi-Kogan 1995, hereafter LRBK95; Yi, Wheeler, & Vishniac 1997) and also for the rotation-period distribution in YSOs (e.g., Königl 1991; Edwards et al. 1993; Bouvier et al. 1993; Collier Cameron & Campbell 1993; Yi 1994, 1995; Ghosh 1995; Collier Cameron, Campbell, & Quaintrell 1995; Herbst et al. 2000). Furthermore, a strong enough field may truncate the disk before it reaches the stellar surface and channel the accretion flow to high stellar latitudes, where it is stopped and thermalized in accretion shocks. This is the accepted explanation for X-ray pulsars (accreting magnetic neutron stars; e.g., Lamb 1989), for DQ Herculis stars (accreting magnetic white dwarfs; e.g., Patterson 1994), and probably also for the optical/UV "hot spots" in classical T Tauri stars (interpreted as accreting magnetic YSOs; e.g., Bertout, Basri, & Bouvier 1988; Königl 1991; Edwards et al. 1994; Hartmann, Hewett, & Calvet 1994; Lamzin 1995; Bertout et al. 1996; Johns-Krull & Basri 1997; Johns-Krull & Hatzes 1997; Martin 1997; Muzerolle, Hartmann, & Calvet 1998).

However, the theory of the interaction between a magnetic star and its accretion disk remains incomplete. One key question is whether a steady state description, adopted in many models, is appropriate. In a Keplerian disk around a star of mass M rotating with angular velocity Ω_*, the gas interior to the *corotation radius* $r_{\rm co} = (GM/\Omega_*^2)^{1/3}$ rotates faster than the star, whereas the matter at $r > r_{\rm co}$ rotates slower. If the star, the disk, and the magnetosphere above it are perfect conductors, then stellar magnetic field lines threading the disk will undergo secular twisting. A steady state can exist only if the twisting of the field lines is countered by the magnetic diffusivity in the disk (e.g., GL). However, in many real cases the disk diffusivity seems to be too small to justify a steady state description (see § 4).

The behavior of twisted magnetic field lines anchored in a well-conducting medium has been first considered in the context of the solar corona both semianalytically (e.g., Aly 1984, 1985, 1995; Low 1986; Low & Lou 1990; Wolfson 1995) and numerically (e.g., Barnes & Sturrock 1972; Klimchuk & Sturrock 1989; Wolfson & Low 1992; Roumeliotis et al. 1994; Mikić & Linker 1994; Amari et al. 1996a, 1996b). Recently, however, there appeared some explicit studies of magnetically linked star-disk systems, again using both semianalytic techniques for force-free configurations (e.g., van Ballegooijen 1994, hereafter VB94; Lynden-Bell & Boily 1994; LRBK95; Bardou & Heyvaerts 1996, hereafter BH96) and full MHD numerical simulations (e.g., Hayashi, Shibata, & Matsumoto 1996; Goodson, Winglee, & Böhm 1997; Miller & Stone 1997; Goodson, Böhm, & Winglee 1999; Goodson & Winglee 1999). These studies have indicated that the applied twist causes a strong expansion of the field lines away from the star. Initially, the evolution is quasi-static, with the azimuthal field building up while the

[1] Also at the Enrico Fermi Institute, University of Chicago.
[2] Dr. Litwin passed away unexpectedly on October 4, 2001. His coauthors wish to dedicate this paper and its companion to his memory.

poloidal field structure changes relatively little, but past a certain point the expansion accelerates rapidly and in a finite time (corresponding to a total twist $\sim\pi$) the system approaches a singular state with at least some of the field lines opened.

As the twisted field lines expand, they become sharply bent at the disk surface and tend to undergo a substantial radial resistive diffusion. Previous studies have either ignored this issue (e.g., LRBK95), or concluded that the magnetic flux would be strongly rearranged and partly expelled from the disk (BH96; Agapitou & Papaloizou 2000), or that the radial field excursions would average to zero (VB94). The resolution of this question depends critically on whether reconnection in the magnetosphere can terminate the field-line expansion before the radial field at the disk surface becomes very large and is thus tied to the field-opening question.

Even if the system is not steady, one could average the relevant quantities over the cycle period (of order the rotation period, see VB94) and use them in modeling effectively steady state star-disk systems (e.g., GL; Zylstra 1988; Daumerie 1996). The time-dependent nature of the magnetic interaction could still be important, however (e.g., Hartmann 1997; Goodson & Winglee 1999), and may, in fact, resolve some of the difficulties with steady state magnetic accretion models (e.g., Safier 1998).

In this paper we address basic issues related to the field opening as well as to the influence of disk resistivity on the evolution of the magnetic field above the disk. In §§ 2 and 3 we study the sequence of force-free equilibria above an *infinitely conducting* thin disk. In § 2 we use a simple, largely semianalytic, approach, based on a sequence of *self-similar* force-free magnetospheric equilibria. In § 3 we generalize our analysis of the opening of magnetic field lines by using a non–self-similar model for a *differentially rotating* disk. In § 4 we clarify the condition for a steady state in a *resistive disk* and also consider the radial migration of flux across the disk. In § 5 we summarize and discuss our results.

In this paper we deliberately do not discuss the possibility of reconnection in the magnetosphere. This important question is addressed in the companion paper (Uzdensky, Königl, & Litwin 2002, hereafter Paper II).

2. PERFECTLY CONDUCTING, UNIFORMLY ROTATING DISK MODEL

In this section we describe a semianalytic model of a force-free magnetic field above a perfectly conducting thin disk. This model, first developed in 1994 by VB94,[3] is relatively simple, and we use it to illustrate the relevant ideas and as a framework for our quantitative analysis.

2.1. *Self-similar Configurations*

Following VB94, we consider a uniformly rotating disk magnetically linked to a central pointlike star. This may be a valid representation of the outer parts of a Keplerian disk, at radii $r \gg r_{\rm co}$, where the beat frequency [the difference $\Delta\Omega$ between the rotation rate $\Omega_d(r)$ of the disk and the rotation rate Ω_* of the star] is almost independent of r (and is equal to $-\Omega_*$). We use spherical coordinates (r, θ, ϕ) and assume axisymmetry. Then the magnetic field can be written in terms of the poloidal flux function $\Psi(r, \theta)$ and the poloidal current F as

$$\boldsymbol{B} = \nabla\Psi \times \nabla\phi + F\nabla\phi \, .$$

The distribution of the poloidal magnetic flux $\Psi_d(r)$ on the surface of an infinitely conducting disk stays fixed as the disk rotates and thus serves as a boundary condition at the disk surface. We are looking for a *self-similar* solution characterized by the absence of a characteristic scale in r. Then, $\Psi_d(r)$ must be a power-law function,

$$\Psi_d(r) = \frac{C}{n} r^{-n} \, , \quad C, n > 0 \, . \tag{2.1}$$

Assuming that the plasma density in the magnetosphere above the disk is low enough for the Alfvén speed $v_{\rm A}$ to greatly exceed both the disk rotation and the sound speeds, the magnetic field at any given time is given by a force-free equilibrium

$$\nabla \times \boldsymbol{B} = \alpha \boldsymbol{B} \, , \tag{2.2}$$

where $\alpha(r, t)$ is a scalar function, constant along each field line.

Since the boundary conditions [i.e., $\Psi_d(r)$] are kept constant, time enters the problem only through the function α.

Following VB94, the self-similar magnetic field can be written as

$$\boldsymbol{B} \equiv [B_r, B_\theta, B_\phi] = \frac{C}{r^{n+2}} \left[f(\theta), \frac{g(\theta)}{\sin\theta}, h(\theta) \right] , \tag{2.3}$$

corresponding to $\Psi(r, \theta) = Cg(\theta)/nr^n$, where the functions $f(\theta)$, $g(\theta)$, and $h(\theta)$ depend also on time. Thus, the assumptions of axisymmetry and self-similarity enable us to reduce the problem to a one-dimensional problem of determining these three functions.

The boundary condition (2.1) implies $g(\pi/2) = 1$, whereas the condition $\nabla \cdot \boldsymbol{B} = 0$ gives

$$f(\theta) = \frac{1}{n \sin\theta} \frac{dg}{d\theta} \, . \tag{2.4}$$

By integrating $dr/d\theta = rB_r/B_\theta$, the shape of the field line is

$$r(\theta, \Psi) = r_0(\Psi)[g(\theta)]^{1/n} \, , \tag{2.5}$$

where $r_0(\Psi)$ is the position of the footpoint of the field line Ψ at the disk surface.

Because of self-similarity, α must scale as $1/r$, i.e., $\alpha(r, t) = a[\theta, \Delta\Phi(t)]/r$, and then the condition $\alpha = {\rm const}$ along $\boldsymbol{B}$ gives

$$\alpha(\Psi, \Delta\Phi) = \frac{a_0(\Delta\Phi)[g(\theta)]^{1/n}}{r} = \frac{a_0(\Delta\Phi)}{r_0(\Psi)} \, . \tag{2.6}$$

Next, the θ component of equation (2.2) relates $h(\theta)$ to $g(\theta)$:

$$h(\theta) = \frac{a_0}{(n+1)\sin\theta} [g(\theta)]^{1+1/n} \, . \tag{2.7}$$

Finally, the ϕ component of equation (2.2) gives the following second-order nonlinear differential equation

[3] A mathematically identical model was constructed independently by Lynden-Bell & Boily (1994) and also, in the solar corona context, by Low & Lou (1990).

for $g(\theta)$:

$$\sin\theta\,\frac{d}{d\theta}\left(\frac{1}{\sin\theta}\,\frac{dg}{d\theta}\right)+n(n+1)g(\theta)+\frac{n}{n+1}\,a_0^2[g(\theta)]^{1+2/n}=0\,. \quad (2.8)$$

The boundary conditions are $g(0)=0$ and $g(\pi/2)=1$.

An equation essentially identical to (2.8) was first derived by Low & Lou (1990) who considered self-similar force-free magnetic fields in the solar corona. They, however, deliberately restricted their analysis to the integer-n case. In addition, their model did not have a conducting disk at the midplane, so the boundary conditions were set at $\theta=0,\ \pi$ instead of $\theta=0,\ \pi/2$ in the present case. Additional requirements of regularity and symmetry (Ψ had to be either symmetric or antisymmetric with respect to $\theta=\pi/2$) then lead to a discrete spectrum of a_0 for each n instead of a continuous spectrum in the VB94 model (see § 2.2).

We note that equation (2.8) can also be obtained directly from the force-free Grad-Shafranov equation

$$\frac{\partial^2\Psi}{\partial r^2}+\frac{\sin\theta}{r^2}\,\frac{\partial}{\partial\theta}\left(\frac{1}{\sin\theta}\,\frac{\partial\Psi}{\partial\theta}\right)=-F(\Psi)F'(\Psi)\,, \quad (2.9)$$

as can be verified by making the self-similar *Ansatz* (2.3) and using equations (2.6)–(2.7). Here the function $F(\Psi)$ on the right-hand side represents the contribution of the toroidal field and is related to $\alpha(\Psi,\ t)$ via

$$\alpha=F'(\Psi)\,. \quad (2.10)$$

Equation (2.8) contains a single parameter (a_0), so the time evolution of the system is described by a one-parameter sequence of equilibria. The dependence of $g(\theta)$ on *time* is parametrized by $a_0(t)$, which, in turn, is implicitly determined by the dependence of the azimuthal twist angle

$$\Delta\Phi(t)=(\Omega_d-\Omega_*)t\equiv\Delta\Omega t \quad (2.11)$$

on a_0. The dependence $\Delta\Phi(a_0)$ can be obtained by integrating the equation $\sin\theta d\phi/d\theta=B_\phi/B_\theta$ along the field, yielding

$$\Delta\Phi=\phi(\pi/2)=\frac{a_0}{n+1}\int_0^{\pi/2}[g(\theta,\ a_0)]^{1/n}\,\frac{d\theta}{\sin\theta}\,. \quad (2.12)$$

2.2. *Magnetic Field Evolution*

For any given a_0, one can integrate equation (2.8) directly and then use equation (2.12) to calculate the corresponding value of $\Delta\Phi$, as was done by VB94. We, however, have reformulated the problem, making $\Delta\Phi$, rather than a_0, the control parameter. This makes the time dependence more transparent: for a given t, $\Delta\Phi$ is given by equation (2.11), and then the problem is solved using $\Delta\Phi$ as the input parameter. This approach also has the merit of expediting the solution process.

To do this, we have replaced $g(\theta)$ by the function $\phi(\theta)$, the twist angle as a function of θ:

$$\phi(\theta)=\frac{a_0}{n+1}\int_0^{\theta}[g(\theta)]^{1/n}\,\frac{d\theta}{\sin\theta}\,. \quad (2.13)$$

The idea here is to express $g(\theta)$ through $\phi(\theta)$ using equation (2.13) and then substitute it into equation (2.8), thus obtaining a differential equation for $\phi(\theta)$. Then the parameter $\Delta\Phi$ comes in via the boundary condition $\phi(\pi/2)=\Delta\Phi$, and a_0 drops out. We have

$$\phi'(\theta)=\frac{a_0}{n+1}\,[g(\theta)]^{1/n}\,\frac{1}{\sin\theta}\,. \quad (2.14)$$

Upon differentiating equation (2.14) two more times, and upon using equation (2.8) to express g'' in terms of g' and g, one finally gets a third-order differential equation for $\phi(\theta)$:

$$\phi'''=(1-n)\,\frac{\phi''^2}{\phi'}+\frac{2\cos^2\theta-n}{\sin^2\theta}\,\phi'-\frac{2n-1}{\tan\theta}\,\phi''-(n+1)\phi'^3\sin^2\theta\,. \quad (2.15)$$

The three boundary conditions are (1) $\phi(0)=0$; (2) $\phi'(0)=0$ [this can be used only if $n<2$: as $\theta\to0$, $g(\theta)\sim\theta^2$, and so $\phi'(\theta)\sim g^{1/n}/\sin\theta\sim\theta^{(2/n)-1}\to0$ if $n<2$]; (3) $\phi(\pi/2)=\Delta\Phi$—a prescribed value.

Once $\phi(\theta)$ is found, a_0 can be derived by using the condition $g(\pi/2)=1$:

$$a_0(\Delta\Phi)=(n+1)\phi'(\pi/2)\,. \quad (2.16)$$

In Figure 1 we plot $a_0(\Delta\Phi)$ for several values of the parameter n. As has been noted by VB94, the dependence of a_0 on $\Delta\Phi$ is nonmonotonic, and for any value of a_0 between 0 and a certain maximal value $a_{0,\,\max}(n)$, there exist two different solutions.[4]

A purely poloidal field ($\Delta\Phi=0$) is potential ($a_0=0$). As the field-line twist $\Delta\Phi$ increases, a_0 grows and reaches a maximum $a_{0,\,\max}$ at $\Delta\Phi_{\max}(n)$. As $\Delta\Phi$ is increased even further, a_0 decreases and eventually vanishes at a certain

[4] Actually, there is an infinite series of bands of values of $\Delta\Phi$ where solutions exist, separated by forbidden bands. Each $\Delta\Phi$ band contains solutions of the same topological class [i.e., solutions with the same number of nodes of $g(\theta)$, with the first band, $0<\Delta\Phi<\Delta\Phi_c$, having zero nodes].

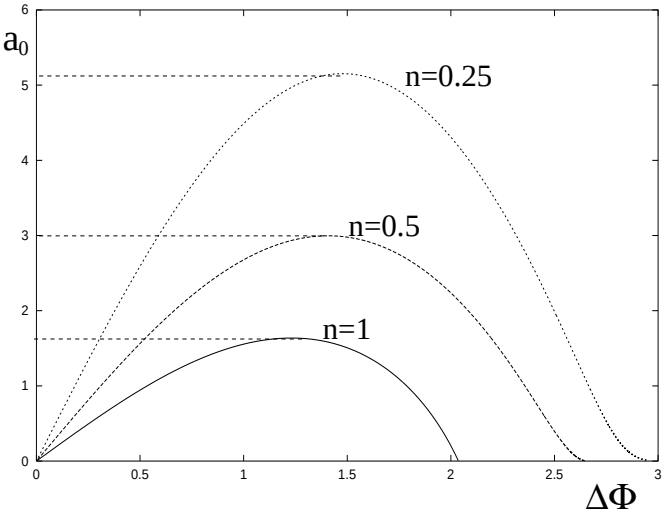

FIG. 1.—Dependence of a_0 on the twist angle $\Delta\Phi$

TABLE 1

PARAMETERS OF THE SELF-SIMILAR MODEL

n	$\Delta\Phi_0$	$\Delta\Phi_{max}$	$a_{0,\,max}$	$h_{d,\,max}$	$\Delta\Phi_c$
1.0	0.00	1.23	1.64	0.82	2.036
0.5	1.05	1.41	3.00	2.00	2.645
0.25.....	1.30	1.48	5.15	4.12	2.944

critical twist angle $\Delta\Phi_c(n)$ [$>\Delta\Phi_{max}(n)$]. We call the $0 < \Delta\Phi < \Delta\Phi_{max}$ part of the curve the ascending branch and the $\Delta\Phi_{max} < \Delta\Phi < \Delta\Phi_c$ part the descending branch. Both $\Delta\Phi_{max}$ and $\Delta\Phi_c$ are, in general, on the order of 1 rad (see Table 1; $\Delta\Phi_0$ is the twist angle for which $f(\pi/2) = 0$; see § 4.2). The nonexistence of solutions for $a_0 > a_{0,\,max}$ agrees with the result obtained by Aly (1984) for his boundary value problem 1, in which one prescribes values of the normal magnetic field B_n and α on the boundary of an infinite domain.

The behavior of the toroidal field at the surface of the disk $B_{d,\phi}$ is given by $h_d(\Delta\Phi) \equiv h(\pi/2, \Delta\Phi) = a_0/(n+1)$ (see eq. [2.7]). Therefore, it also first increases nearly linearly with $\Delta\Phi$ and reaches a maximum $h_{d,\,max} = a_{0,\,max}/(n+1)$ at $\Delta\Phi = \Delta\Phi_{max}$. After that, the built-up magnetic stress causes the flux tubes to expand rapidly and to become elongated along the direction of the apex angle θ_{ap} (see Fig. 2).[5] The field-line twist travels out to the apex of the flux tube, where the field is weakest, which can be understood in terms of torque balance along the tube (e.g., Parker 1979). At the same time $B_{d,\phi}$ decreases and goes to zero at $\Delta\Phi = \Delta\Phi_c$. The fact that $B_{d,\phi}$ remains bounded as the twist increases is central to our analysis of the evolution of resistive disks (§ 4.1).

2.3. *Finite-Time Singularity*

As the critical twist angle $\Delta\Phi_c$ is approached (and $a_0 \to 0$), the solution of equations (2.8) and (2.15) blows up, with the field lines expanding to infinity and thus opening up (see Fig. 2). The radial field component at the disk surface diverges, whereas the surface azimuthal field goes to zero. No solutions exist for $\Delta\Phi > \Delta\Phi_c$. This behavior is generic to twisted flux tubes and is characterized as a "finite time singularity" (e.g., Aly 1995): the magnetic field reaches a singular state after being twisted for a finite time (or, equivalently, by a finite angle).

To analyze the asymptotic ($a_0 \to 0$) properties of the function $g(\theta)$, we note that a_0 can be rescaled out of equation (2.8) by the substitution

$$G(\theta) = g(\theta) a_0^n \,. \tag{2.17}$$

The equation for $G(\theta)$ is

$$\sin\theta \frac{d}{d\theta}\left(\frac{1}{\sin\theta}\frac{dG}{d\theta}\right) + n(n+1)G(\theta) + \frac{n}{n+1}[G(\theta)]^{1+2/n} = 0 \,. \tag{2.18}$$

The boundary conditions are $G(0) = 0$ and $G(\pi/2) = a_0^n$. Thus, the parameter a_0 has moved from the equation to a boundary condition. The transition to the limit $a_0 \to 0$ can now be easily made, since the solution of equation (2.18) does not blow up as the boundary condition at $\theta = \pi/2$ approaches zero. We designate the solution of equation (2.18) with the boundary conditions $G(0) = G(\pi/2) = 0$ as $G_0(\theta)$. This function depends only on n and remains finite in the entire interval $(0, \pi/2)$ (see Fig. 3). The behavior of the original function $g(\theta)$ near $\Delta\Phi_c$ is given by

$$g(\theta, a_0, n) \to G_0(\theta, n) a_0^{-n} \quad \text{as } a_0 \to 0 \,. \tag{2.19}$$

This solution has a number of useful implications. First, by combining equations (2.12) and (2.19), one can calculate the critical twist angle $\Delta\Phi_c$:

$$\Delta\Phi_c = \frac{1}{n+1}\int_0^{\pi/2} G_0^{1/n}(\theta)\frac{d\theta}{\sin\theta} \,. \tag{2.20}$$

Second, as shown in Figure 3, the apex angle θ_{ap}, at which $G_0(\theta)$ reaches its maximum, is very close to 60° for a wide range of values of n. In fact, $\theta_{ap} \to 60°$ as $n \to 0$, in agreement with the finding by Lynden-Bell & Boily (1994). The azi-

[5] The apex θ_{ap} is defined as the most distant from the star point on a field line. According to equation (2.5), this is also the point of maximum of $g(\theta)$.

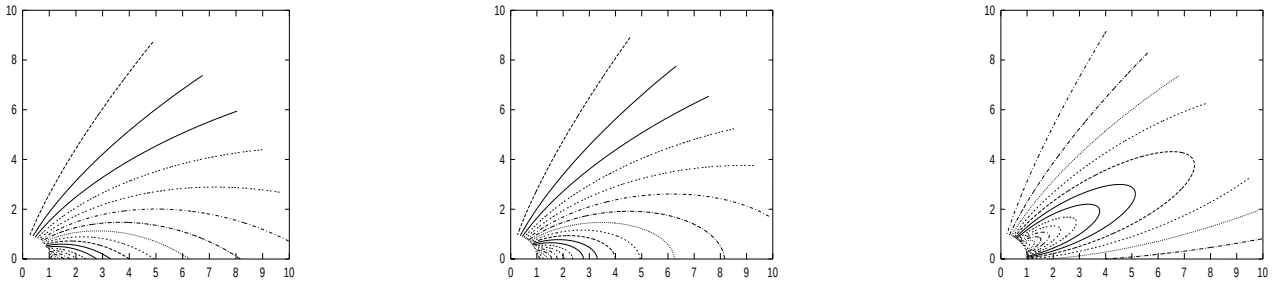

FIG. 2.—Meridional projection of the magnetic field lines for three values of the twist angle $\Delta\Phi$ in the case $n = 0.5$, plotted in the (arbitrarily chosen) interval $r \in [1, 10]$.

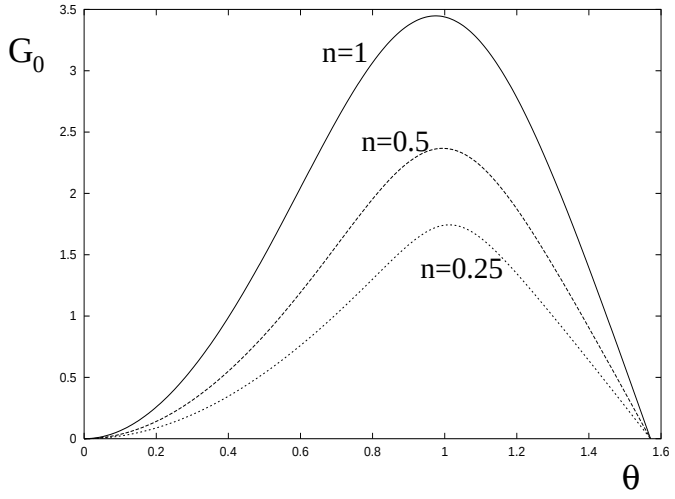

FIG. 3.—Plots of the function $G_0(\theta)$ for three values of n

muthal current density in the magnetosphere, which is related to $g(\theta)$ via equations (2.2), (2.3), (2.6), and (2.7), is also concentrated around this angle, and in the limit $n \ll 1$ the current distribution collapses into a narrow layer that extends radially along $\theta \approx \theta_{ap}$ (see Fig. 4). As we discuss in our Paper II, such a current layer is a natural potential site for rapid field reconnection in the magnetosphere. Third, similar to j_ϕ, the azimuthal flux is also concentrated near the angle θ_{ap} (see eq. [2.7]). This is a manifestation of the outward propagation of the magnetic field twist discussed in § 2.2.

3. KEPLERIAN DISK

The analysis in the previous section employed the self-similar solution. In this section we examine the more realistic case of a Keplerian disk and compare it with the self-similar model. Since the Keplerian disk has a characteristic radial scale (the corotation radius r_{co}), the self-similar semianalytic approach is clearly inapplicable. The problem becomes fully two-dimensional and requires numerical tools.

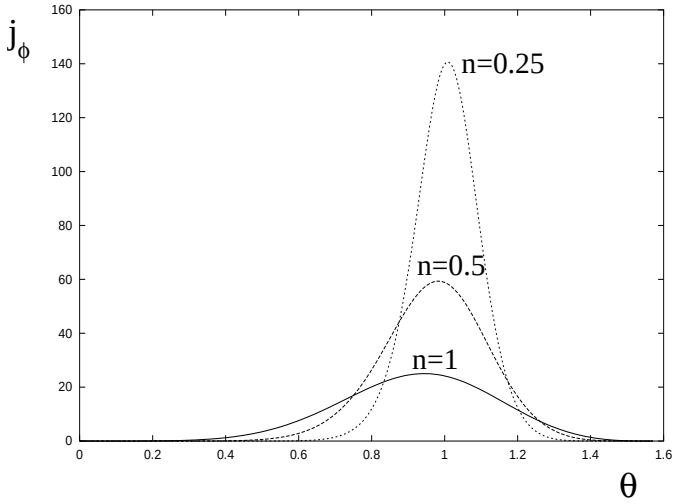

FIG. 4.—Plots of the azimuthal current density $j_\phi(\theta)$ in the limit $\Delta\Phi \to \Delta\Phi_c$ for three values of n.

We developed a numerical code that enables us to find sequences of equilibria once the rotation law, $\Delta\Omega(r)$, and the poloidal magnetic flux, $\Psi_d(r)$, are specified on the disk surface. (In contrast to the self-similar case, these two functions no longer have to be power laws.) We first describe the numerical procedure and then present the results of our computations.

The computational domain consists of the outside of a sphere of radius R_* (see Fig. 5). In the remainder of this section, we normalize the radius r by R_*. Using the symmetry with respect the disk plane, we consider only the upper halfspace.

To find the force-free equilibria, we solve the Grad-Shafranov equation

$$\frac{\partial^2\Psi}{\partial r^2} + \frac{\sin\theta}{r^2}\frac{\partial}{\partial\theta}\left(\frac{1}{\sin\theta}\frac{\partial\Psi}{\partial\theta}\right) = -F(\Psi)F'(\Psi)\,. \quad (3.1)$$

The main difficulty here is that the nonlinear term on the right-hand side $[F(\Psi)F'(\Psi)]$ is not given explicitly. Rather, it is determined implicitly by the rotation law via the condition

$$\Delta\Phi(\Psi) = \Delta\Omega(\Psi)t = F(\Psi)I(\Psi)\,, \quad (3.2)$$

where $I(\Psi)$ is an integral along the magnetic field line Ψ

$$I(\Psi) \equiv \int_\Psi \frac{1}{rB_\theta}\frac{d\theta}{\sin^2\theta}\,. \quad (3.3)$$

The time t in equation (3.2) is the parameter controlling the sequence of equilibria, and the rotation law $\Delta\Omega[\Psi_d(r)]$ is a prescribed function. For example, $\Delta\Omega = -\Omega_* \times [1 - (r_{co}/r)^{3/2}]$ for a Keplerian disk. In the remainder of this section, we normalize t by $|\Omega_*|^{-1}$.

Our goal is to find the time sequence of equilibria for a given rotation law. We start at $t = 0$ with the potential field corresponding to $F \equiv 0$ and then step through the sequence by calculating equilibria separated by small time increments. For each moment t we solve the system (3.1)–(3.3) iteratively: at the kth iteration we plug the result $F^{(k)}(\Psi)$ of the previous iteration into the right-hand side of

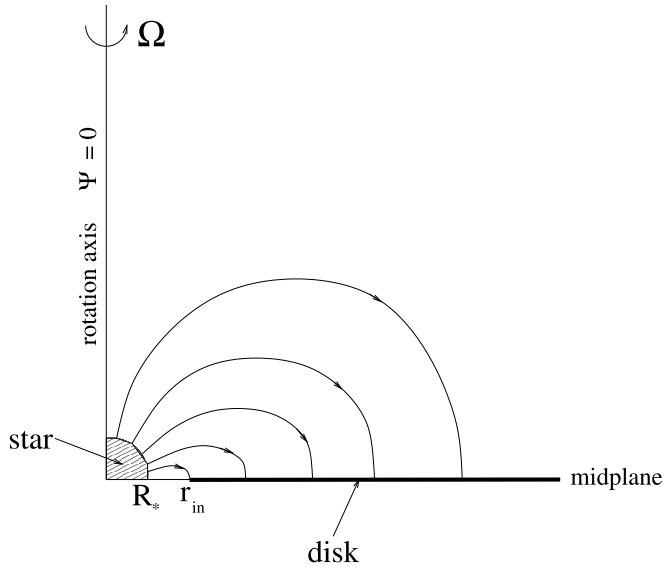

FIG. 5.—Geometry of the problem

equation (3.1) [taking $F^{(0)}(\Psi)$ to be the solution for the previous moment of time, or zero for $t = 0$], solve equation (3.1), then use the solution $\Psi^{(k)}(r, \theta)$ to calculate the integral $I^{(k)}(\Psi)$ along field lines, and then we update the function $F(\Psi)$ according to

$$F^{(k+1)}(\Psi) = \Delta\Omega(\Psi)t/I^{(k)}(\Psi) . \tag{3.4}$$

We repeat this procedure until the process converges.[6]

When solving the elliptic equation (3.1) for given t and k, we use the relaxation method. We introduce a fictitious time variable τ and then evolve $\Psi(\tau, r, \theta)$ according to

$$\frac{\partial\Psi}{\partial\tau} = \frac{\partial^2\Psi}{\partial r^2} + \frac{\sin\theta}{r^2}\frac{\partial}{\partial\theta}\left(\frac{1}{\sin\theta}\frac{\partial\Psi}{\partial\theta}\right) + F(\Psi)F'(\Psi) . \tag{3.5}$$

If one uses a uniform grid in spherical coordinates (r, θ), one has to introduce an outer boundary at some large radius $r = r_{\max}$. At this boundary one runs into serious problems related to boundary conditions and the treatment of the integral (3.3) for field lines crossing this boundary. To bypass these issues, we effectively place the outer boundary at infinity by using the transformation

$$x = \frac{1}{\sqrt{r}} , \tag{3.6}$$

which maps $r = \infty$ to $x = 0$ while keeping the inner boundary (the surface of the star $R_* = 1$) at $x = 1$. Correspondingly, we replace the uniform (r, θ) grid with a uniform (x, θ) one. Then, equation (3.5) becomes

$$\frac{\partial\Psi}{\partial\tau} = \frac{1}{4}x^6\frac{\partial^2\Psi}{\partial x^2} + \frac{3}{4}x^5\frac{\partial\Psi}{\partial x} + x^4\sin\theta\frac{\partial}{\partial\theta}\left(\frac{1}{\sin\theta}\frac{\partial\Psi}{\partial\theta}\right) + F(\Psi)F'(\Psi) . \tag{3.7}$$

This equation is integrated on a rectangular domain $x \in [0,1]$, $\theta \in [0, \pi/2]$. There are four boundaries: the surface of the star $x = 1$, the axis $\theta = 0$, the outer boundary $x = 0$, and the surface of the disk $\theta = \pi/2$. On three of these the boundary conditions are particularly simple:

$$\Psi(x, \theta = 0) = \Psi(x = 0, \theta) = 0 , \tag{3.8}$$

$$\Psi(x = 1, \theta) = \Psi_*(\theta) , \tag{3.9}$$

where $\Psi_*(\theta)$ is the magnetic flux distribution on the surface of the (infinitely conducting) star, which we take to be

$$\Psi_*(\theta) = \sin^2\theta , \tag{3.10}$$

which corresponds to the dipole field.

The boundary conditions on the equatorial plane $\theta = \pi/2$ are more complicated because of the inner gap between the disk and the star (see Fig. 5). Typically we place the inner edge of the disk at $r_{\rm in} = 1.5$ (so that $x_{\rm in} = \frac{2}{3}$, $\Psi_{\rm in} = \frac{2}{3}$). The space inside the gap, $1 < r < r_{\rm in}$, is filled with very tenuous plasma, just like the magnetosphere above the disk. Hence, the field lines going through the gap must be potential, and, because of the symmetry with respect to the midplane, perpendicular to this plane

$$\frac{\partial\Psi}{\partial\theta}\left(x > x_{\rm in}, \theta = \frac{\pi}{2}\right) = 0 . \tag{3.11}$$

In the region $r > r_{\rm in}$ the magnetic field lines are frozen into the disk surface; hence, the flux distribution there is a prescribed function, which we take to be a dipole,

$$\Psi\left(x < x_{\rm in}, \theta = \frac{\pi}{2}\right) = \Psi_d(x) = x^2 = \frac{1}{r} . \tag{3.12}$$

We start with the potential dipole field at $t = 0$ and then proceed through the sequence by gradually increasing t (and so the twist angle) and by using the solution for the previous value of t as the initial guess for the next value of t. For numerical convenience, we want $\Delta\Omega(r)$ to go smoothly to zero at $r_{\rm in}$ (which also makes physical sense, since near the inner gap the gas undergoes a gradual transition from a Keplerian rotation to corotation with the star). Along the rest of the disk surface, however, $\Delta\Omega(r)$ can be arbitrary. We investigated two cases: *uniform rotation* (Fig. 6*a*), wherein $\Delta\Omega(r) \to$ const for $r \gg r_{\rm in}$, and *Keplerian rotation* (Fig. 6*b*), where, for $r > r_{\rm in}$, the rotation law approaches Keplerian with $r_{\rm co} = 6$.

We now turn to a description of our results. Figures 7 and 8 show a series of magnetic contour plots for several values of t for the uniformly rotating and Keplerian disk

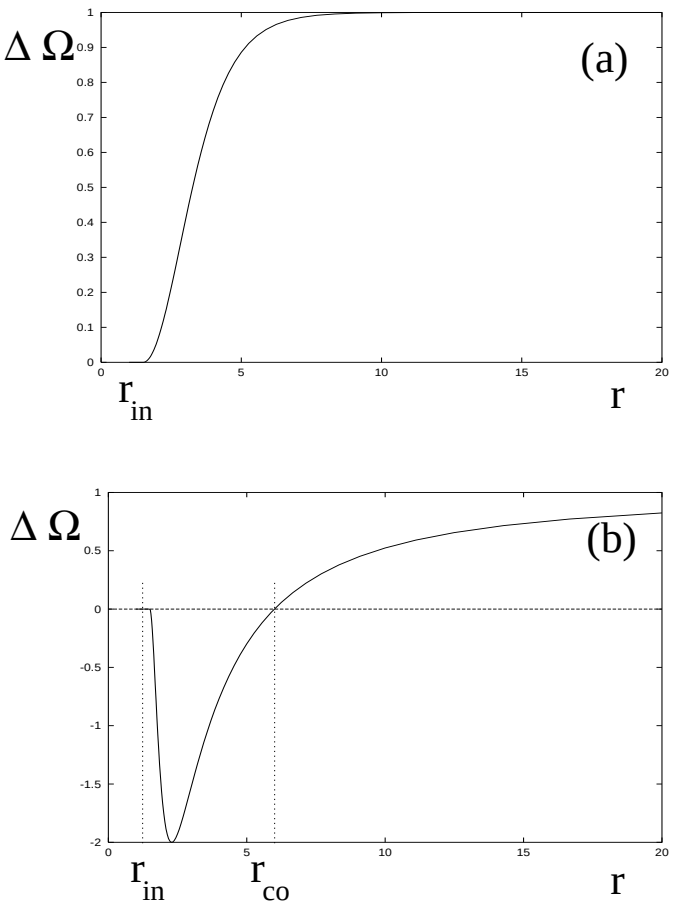

FIG. 6.—Angular velocity profile $\Delta\Omega(r)$ for (*a*) uniformly rotating disk and (*b*) Keplerian disk.

[6] Our approach is different from that of Agapitou & Papaloizou (2000) in the important respect that they did not have to calculate $F(\Psi)$ from the conditions (3.2)–(3.3). Instead, they calculated $F(\Psi)$ directly from $F = B_{d,\phi}r$ using the steady state expression (4.3) for $B_{d,\phi}$. Thus, their solutions are valid only for the steady state of a resistive disk discussed in § 4, whereas ours describe the entire time evolution in the case of a conducting disk.

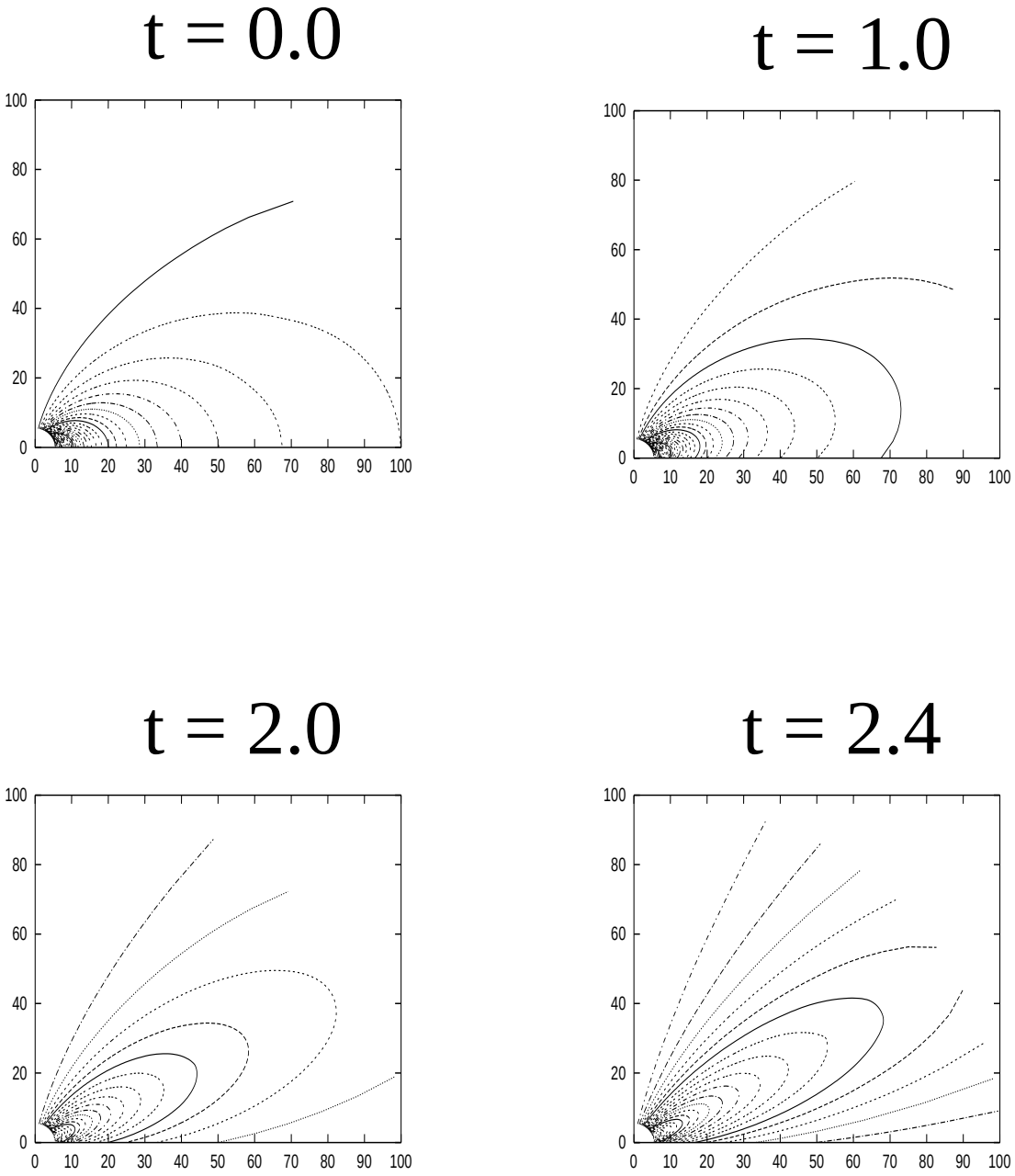

FIG. 7.—Sequence of magnetic field contours for the uniformly rotating disk model

models, respectively. In both cases, the basic behavior (i.e., the rapid expansion of the field lines near $\theta \simeq 60°$–$70°$) is very similar. Figures 9 and 10 describe the evolution of $F(\Psi, t)$ for the two cases. Generally, the evolution can be divided into two stages, distinguished by the time behavior of $F(\Psi, t)$ on the field line with the largest twist. For the Keplerian disk, this field line is given by $\Psi_1 = 0.44$, on which $|\Delta\Phi|$ is twice the asymptotic value at infinity (see Fig. 6*b*). Note that the function $F(\Psi = \Psi_1, t)$, shown in Figure 11, serves as an indirect analog of $a_0(\Delta\Phi)$ in the self-similar model.

In the uniform-rotation disk model the analogy can be made more direct by looking at the evolution of $d^2F(\Psi)/d\Psi^2$ at $\Psi = 0$. Indeed, at large distances, $r \gg r_{\rm in}$, the twist angle $\Delta\Phi$ approaches a constant (see Fig. 6*a*), so one can expect a self-similar power-law asymptotic behavior for $F(\Psi)$ in the limit $\Psi \to 0$. Using $\alpha(\Psi) = F'(\Psi)$ and $F(0) = 0$, one can express $F(\Psi, t)$ using the notation of § 2.1 as

$$F(\Psi, t) = \int_0^{\Psi} \alpha d\Psi = \int_0^{\Psi} \frac{a_0(t) d\Psi}{r_0(\Psi)} = \frac{a_0(t)\Psi^2}{2}, \quad \Psi \to 0, \tag{3.13}$$

where we used equation (3.12). This quadratic behavior is indeed exhibited by our calculated solution. Thus, we select the time evolution of

$$a_0(t) \equiv \left. \frac{d^2F}{d\Psi^2} \right|_{\Psi = 0} \tag{3.14}$$

for a direct comparison with the self-similar model. Figure 12 demonstrates that on the ascending branch of the solution the agreement is very good, while on the descending branch there is some deviation, particularly in the value of

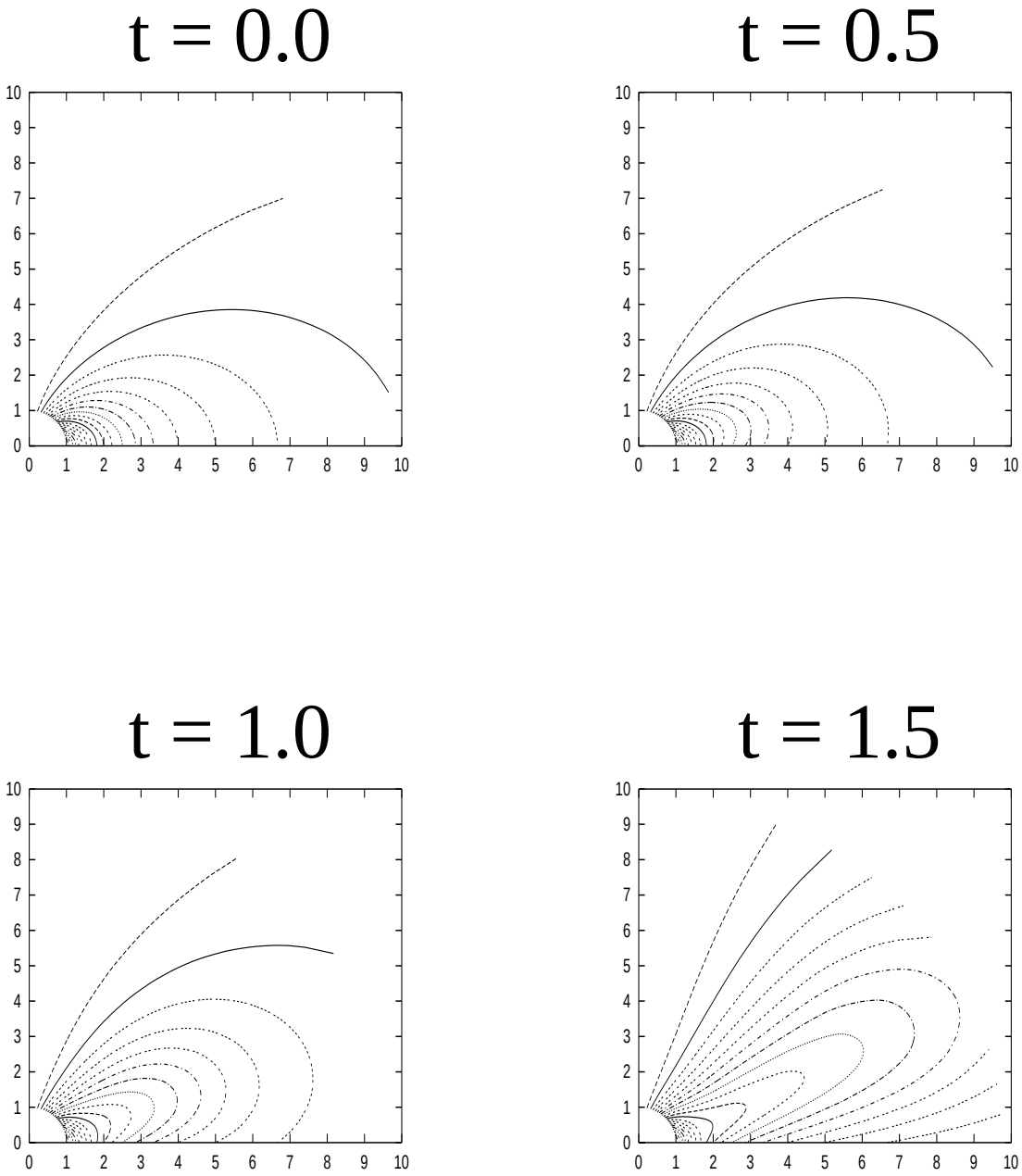

FIG. 8.—Sequence of magnetic field contours for the Keplerian disk model

$\Delta\Psi_c$. This is because the innermost field lines have smaller twist and therefore are not inflated as much as in the self-similar case. Hence, the magnetic stresses driving the expansion are weaker, and the opening of the field is delayed. Still, we see that the basic behavior is the same. As t is increased, $a_0(t)$ (and $|F(\Psi_1, t)|$ in the Keplerian case) rises, reaches a maximum at some $t_{\max}$, and then decreases, just as in the self-similar model. Since $F(\Psi) = B_{d,\phi}(\Psi)r_0(\Psi)$, the evolution of the toroidal field at the disk surface traces that of $F(\Psi, t)$ for a given Ψ. During the first stage ($t < t_{\max}$), the shape of the field lines does not change much, but during the second stage ($t > t_{\max}$), there is a rapid expansion of the field lines, which approach an open state (see Figs. 7 and 8). This qualitative behavior is consistent with the conclusions of Roumeliotis et al. (1994). Also, we find that this behavior is very robust and independent of the details, such as the particular shape of $\Delta\Omega(r)$. However, some quantitative features, such as the values of $t_{\max}$ and $a_{0,\max}$ [or $F(\Psi_1, t_{\max})$] do depend on the particular parameters ($r_{\rm in}$, $r_{\rm co}$, Ψ_1, etc.).

These two stages also have very different numerical convergence properties. During the first stage the convergence is rapid and robust, but during the second stage it slows down, one has to update $F(\Psi)$ more often, and finally one has to stop the computation at some point. Fortunately, by this time the field lines have expanded so drastically (see Figs. 13 and 14) that an extrapolation of the $a_0(t)$ and $F(\Psi_1, t)$ becomes possible. We deduce that these functions reach zero at a finite twist angle, implying a field-line opening in a finite time, similar to the self-similar model. We estimate the critical twist angle to be about 2.7 rad for the uniform-rotation case and 4.0 rad (corresponding to $t = 2.0$; see Fig. 6*b* for the Keplerian case).

Thus, a good case can be made for the finite-time singularity for a broad class of models. To strengthen this point,

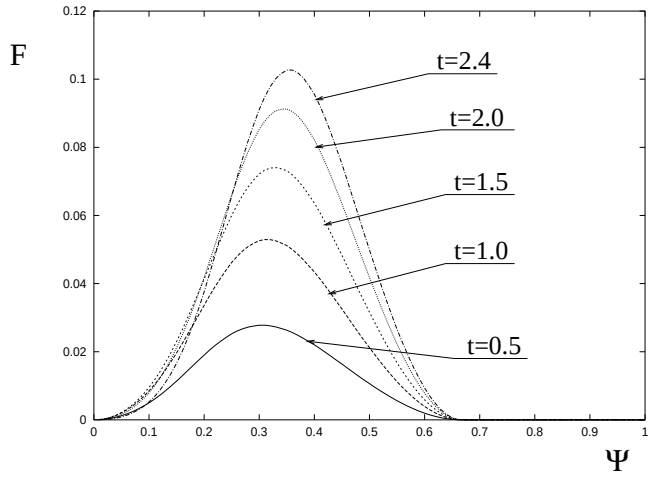

FIG. 9.—$F(\Psi, t)$ for the uniformly rotating disk model

we propose the following simple physical argument (different from Aly 1995).

Consider the small-F limit of equation (3.1), in which the nonlinear term $FF'(\Psi)$ is smaller than, say, the first linear term on the left-hand side at typical distances $r \sim r_0(\Psi)$.

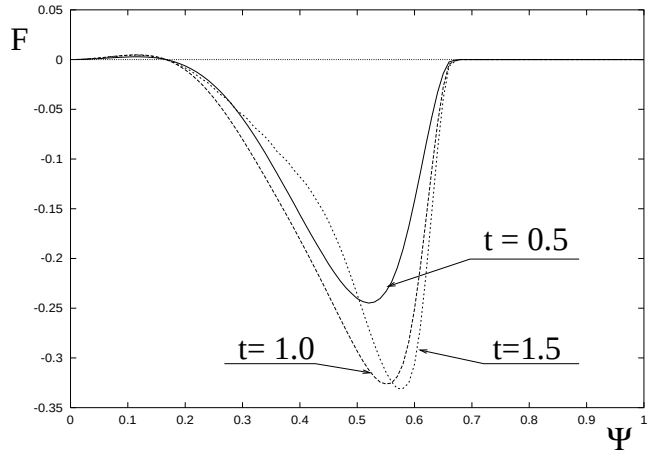

FIG. 10.—$F(\Psi, t)$ for the Keplerian disk model

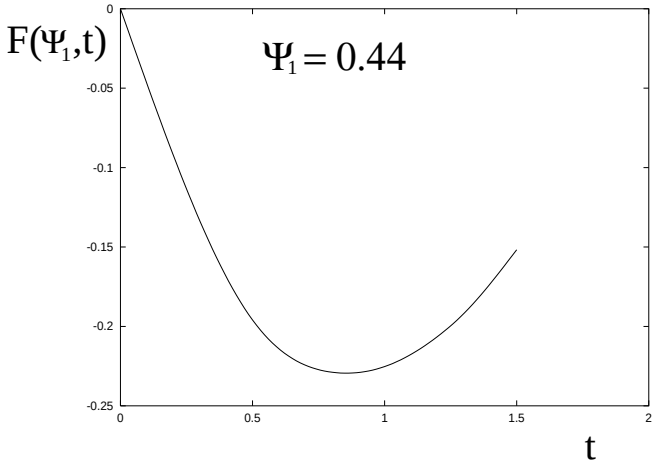

FIG. 11.—Evolution of the function $F(\Psi_1, t)$ for the Keplerian disk model; $\Psi_1 = 0.44$ is the field line with the largest twist.

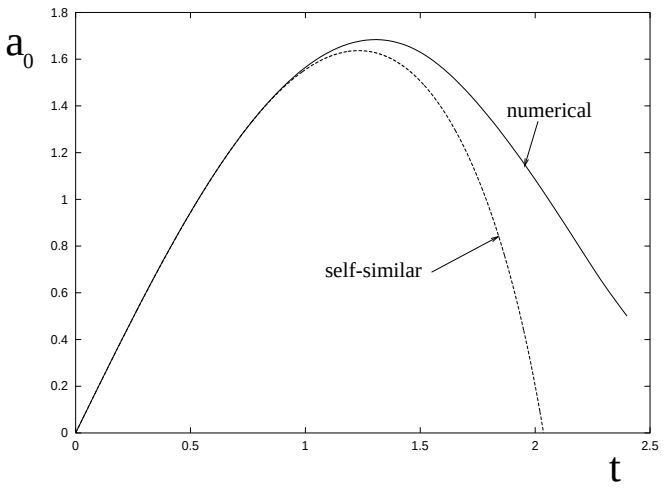

FIG. 12.—Function $a_0(t)$ (eq. [3.14]) for the uniformly rotating disk. The solid line shows the result of our numerical calculations, whereas the dashed line shows the behavior of $a_0(t)$ in the self-similar model of § 2.

Dimensional analysis then gives

$$F(\Psi) \ll \frac{\Psi}{r_0(\Psi)} . \tag{3.15}$$

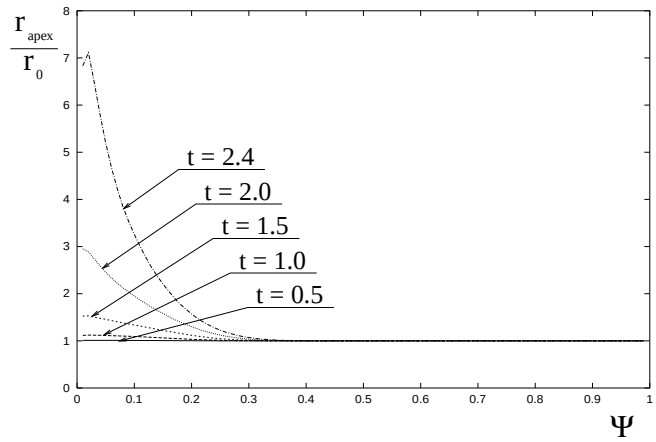

FIG. 13.—Expansion factor as a function of magnetic flux in the uniformly rotating disk model.

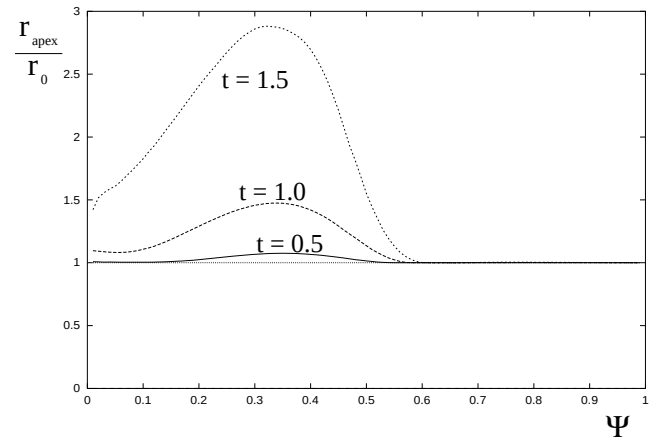

FIG. 14.—Expansion factor as a function of magnetic flux in the Keplerian disk model.

Small values of F may correspond to two qualitatively different solutions. The first one is close to the potential field, with the nonlinear term being unimportant everywhere on the field line. The other solution describes greatly expanded field lines that stretch out far enough for the linear terms (of order Ψ/r^2) to become small, so that the nonlinear term gives an important contribution on the distant portion of these field lines. For a given value of F, we can then define a characteristic radial scale r_F,

$$r_F(\Psi, t) \equiv \frac{\Psi}{F(\Psi, t)} \gg r_0(\Psi) . \tag{3.16}$$

This expression gives an estimate of the position $r_{\rm ap}(\Psi, t)$ of the apex of the field line Ψ. It also enables us to evaluate the twist angle of the field line Ψ at time t. Using equations (3.2) and (3.3) and *assuming* that in the θ direction there are no thin scales (i.e., current sheets), we obtain

$$\Delta\Phi(\Psi, t) = F(\Psi, t) \int_{\Psi} \frac{d\theta}{B_\theta r(\Psi, \theta) \sin^2 \theta} \sim F(\Psi, t) \frac{1}{(B_\theta r)_{\rm min}} . \tag{3.17}$$

Now $(B_\theta r)_{\rm min} = -[(\partial\Psi/\partial r)/\sin\theta]_{\rm min}$ can be estimated simply as $(\Psi/r)_{\rm min} = \Psi/r_{\rm ap}(\Psi, t) \sim \Psi/r_F$. Thus,

$$\Delta\Phi(\Psi, t) \sim F(\Psi, t) \frac{r_F}{\Psi} \sim O(1) . \tag{3.18}$$

Therefore, as $F \to 0$ and the field lines open, $\Delta\Phi$ approaches a finite value independent of F, and one encounters a finite-time singularity.

4. STEADY STATE CONFIGURATIONS

In this section we consider the conditions under which a magnetically linked star-disk configuration can reach a steady state. We continue to assume, as in § 2, that both the star and the magnetosphere are perfect conductors, but we allow the disk to have a finite resistivity. For ease of presentation, we use the self-similar model outlined in § 2, which corresponds to a uniformly rotating disk. Self-similarity imposes a condition on the radial dependence of the vertically integrated electrical conductivity Σ. However, since our analysis is essentially local, we expect the basic conclusions to remain valid also in the general case of a differentially rotating disk and a non–self-similar diffusivity. To further simplify the presentation, we first consider the case where the radial positions of the field lines in the disk remain fixed during the twisting process, so the diffusivity acts only in the azimuthal direction. We then also examine the consequences of the radial field diffusion.

4.1. *Time Evolution of the Twist Angle*

We first derive the time evolution of the twist angle for a thin resistive disk. The normal field component at the disk surface is given approximately by $B_{d,z} \equiv B_z(z = H) \approx B_z(z = 0) = -B_\theta(r, \pi/2)$, where $2H \ll r$ is the disk's thickness. Then, since $B_\phi(z = 0) = 0$ owing to the reflection symmetry, the radial surface current density $K_r \approx 2Hj_r(z = 0)$ can be written as $K_r = -cB_{d,\phi}/2\pi$. But, by Ohm's law, it is related to the radial electric field at the disk surface by $E_{d,r} = K_r/\Sigma - v_{d,\phi} B_{d,z}/c$, where $v_{d,\phi} \equiv r\Omega_d$ and Σ is related to the magnetic diffusivity η through $\Sigma \approx Hc^2/2\pi\eta$. On the other hand, the azimuthal speed of the field lines at the midplane is $v_{B,\phi} = -cE_{d,r}/B_{d,z}$. Relative to the disk matter, this speed is $v_{B,\phi} - v_{d,\phi} = -cK_r/\Sigma B_{d,z} \approx \eta B_{d,\phi}/HB_{d,z}$. Thus, the time evolution of the twist angle is given by

$$\frac{d\Delta\Phi}{dt} = \Delta\Omega + \frac{c^2}{2\pi r\Sigma} \frac{B_{d,\phi}}{B_{d,z}} . \tag{4.1}$$

The first term on the right-hand side of equation (4.1) represents the secular growth of $\Delta\Phi$ owing to the differential rotation between the disk and the star, whereas the second term (in which $c^2/2\pi\Sigma \approx \eta/H$) describes the azimuthal resistive slippage of the field lines relative to the disk material. This result is quite general and depends only on the disk being thin and on the magnetosphere being perfectly conducting; no other assumptions (such as equilibrium in the magnetosphere) need to be made.

In general, the ratio $B_{d,\phi}/B_{d,z}$ is a function of $\Delta\Phi$ determined uniquely by the solution in the magnetosphere. Then, for a given distribution of $\Sigma(r)$, one obtains a closed equation for $\Delta\Phi(r, t)$. For example, consider the self-similar model discussed in § 2. Self-similarity will not be violated by resistive effects if we demand that $\Sigma(r) \propto 1/r$. In that case $B_{d,\phi}/B_{d,z}(\Delta\Phi) = -h(\pi/2, \Delta\Phi) = -a_0(\Delta\Phi)/(n + 1)$ (see eq. [2.7]), so equation (4.1) becomes

$$\frac{d\Delta\Phi}{dt} = \Delta\Omega - \frac{c^2}{2\pi r\Sigma} \frac{a_0(\Delta\Phi)}{n + 1} . \tag{4.2}$$

Equation (4.1) gives a unique value of the azimuthal field at the disk surface required for maintaining a steady state,

$$B_{\phi,\rm ss} = -\frac{2\pi r\Sigma\Delta\Omega}{c^2} B_{d,z} . \tag{4.3}$$

This result for $B_{\phi,\rm ss}$ or a variation thereof was previously obtained and discussed by a number of authors (e.g., GL; Campbell 1992; LRBK95; BH96; Agapitou & Papaloizou 2000; Wang 1987).

Let us now ask: when will a particular system with a given disk surface conductivity $\Sigma(r)$ and differential rotation rate $\Delta\Omega(r)$ be able to attain a steady state? As an illustration, consider a self-similar force-free magnetosphere. As we know from § 2.2, $|B_{d,\phi}(\Delta\Phi)|$ at first grows with increasing $\Delta\Phi$, reaches a maximum $|B_{d,\phi}^{\rm max}|$ at $\Delta\Phi_{\rm max}$, and then declines to zero at $\Delta\Phi_c$. We thus see that whether or not a steady state can be reached depends on the relative magnitude of $B_{d,\phi}^{\rm max}$ and $B_{\phi,\rm ss}$.

We define a maximum surface conductivity $\Sigma_{\rm max}$ by

$$\Sigma_{\rm max} = \left| \frac{c^2}{2\pi r\Delta\Omega} \frac{B_{d,\phi}^{\rm max}}{B_{d,z}} \right| = \left| \frac{c^2}{2\pi r\Delta\Omega} \right| h_{d,\,\rm max} , \tag{4.4}$$

where the second equality gives the result for our self-similar model. If $\Sigma > \Sigma_{\rm max}$, then $|B_{d,\phi}^{\rm max}| < |B_{\phi,\rm ss}|$ and there is *no steady state*: the azimuthal resistive slippage is not strong enough to counter the twisting, and a singularity is reached in a finite time (corresponding to $\Delta\Phi_c$). Resistive diffusion merely delays the onset of the singularity but does not remove it. The resistive time delay Δt increases with decreasing Σ, as shown in Figure 15. The slowdown rate is largest near $\Delta\Phi_{\rm max}$ where $|B_{d,\phi}|$, and hence the azimuthal resistive slippage, are maximized. As the critical twist $\Delta\Phi_c$ is approached, the time derivative of $\Delta\Phi$ reverts to its initial value $\Delta\Omega$ because $|B_{d,\phi}|$ vanishes at the singular point.

Conversely, if $\Sigma < \Sigma_{\rm max}$, then $B_{d,\phi}^{\rm max} > B_{\phi,\rm ss}$, and *a steady state can be reached*, as shown in Figure 16. If one starts with a purely poloidal field ($\Delta\Phi = 0$, $B_{d,\phi} = 0$), then $\Delta\Phi$

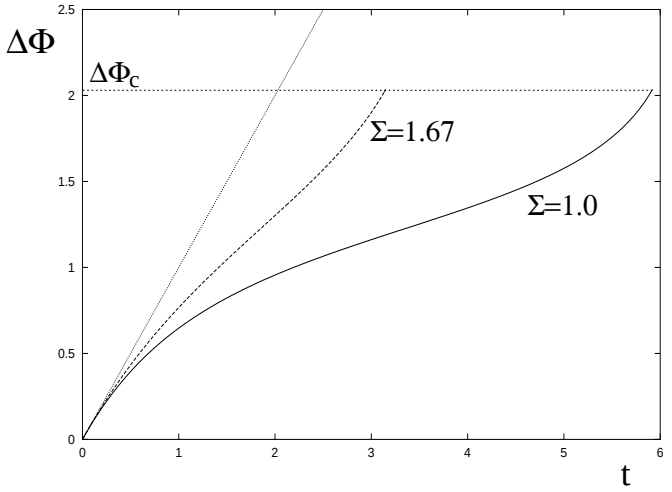

FIG. 15.—Time evolution of the twist angle for several values of the disk surface conductivity Σ above $\Sigma_{\rm max}$ (eq. [4.4]) in the $n = 1$ self-similar solution. The time t is given in units of $1/\Delta\Omega$ and the surface conductivity in units of $c^2/2\pi\Delta\Omega r$ ($\Sigma_{\rm max}$ in these units is equal to $h_{d,\,\rm max} = 0.82$). The slanted dotted line marks the initial phase of the evolution.

initially grows linearly with time but then asymptotically approaches the steady state value $\Delta\Phi_{\rm ss}$ defined by

$$B_{d,\phi}(\Delta\Phi_{\rm ss}) = B_{\phi,\rm ss}\ . \tag{4.5}$$

Note that, although two solutions exist for any given value of $|B_{d,\phi}| < |B_{d,\phi}^{\rm max}|$, the steady state corresponding to the left (ascending) branch ($\Delta\Phi_{\rm ss} < \Delta\Phi_{\rm max}$) is stable, whereas the one corresponding to the right (descending) branch ($\Delta\Phi_{\rm ss} > \Delta\Phi_{\rm max}$) is unstable. Indeed, suppose we are at some steady state and decrease $\Delta\Phi$ slightly. Then, if $\Delta\Phi < \Delta\Phi_{\rm max}$, $|B_{d,\phi}|$ decreases, and the azimuthal slippage becomes smaller than $\Delta\Omega r$, causing $\Delta\Phi$ to rise back to its original value. If, however, $\Delta\Phi > \Delta\Phi_{\rm max}$, then, as $\Delta\Phi$ is decreased, $|B_{d,\phi}|$ will increase, and the enhanced azimuthal resistive slippage will cause $\Delta\Phi$ to drop even further, moving away from the original state.

Let us now ask: can real magnetically linked star-disk systems be expected to reach a steady state? Magnetic diffusivity in astrophysical plasmas is often ascribed to an anomalous resistivity produced by fluid turbulence (e.g., Parker 1979). Here we shall follow the standard α-prescription that

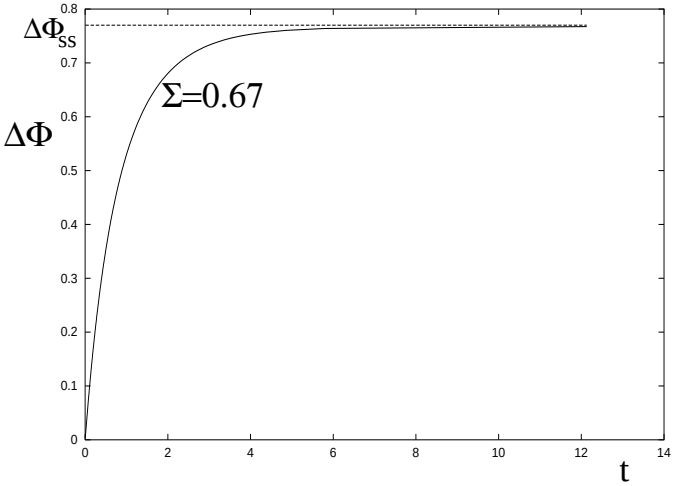

FIG. 16.—Time evolution of the twist angle in the $n = 1$ self-similar solution for the case in which the disk surface conductivity is less than $\Sigma_{\rm max}$. The normalizations of t and of Σ are the same as in Fig. 15.

Shakura & Sunyaev (1973) have introduced to describe the effective anomalous viscosity in turbulent accretion disks. They have estimated the turbulent viscosity as $\nu_{\rm turb} = \alpha c_s H$, where $\alpha = {\rm const} \lesssim O(1)$. Following this methodology, we introduce a constant $\beta \lesssim O(1)$ and write the turbulent magnetic field diffusivity as $\eta_{\rm turb} = \beta c_s H$. Then the effective surface conductivity is

$$\Sigma \approx \frac{c^2}{2\pi\beta c_{\rm s}}\ , \tag{4.6}$$

so

$$\frac{\Sigma}{\Sigma_{\rm max}} \approx \left(\frac{1}{\beta h_{d,\,\rm max}}\right)\frac{r\Delta\Omega}{c_{\rm s}}\ , \tag{4.7}$$

which is $\gg 1$ in a thin disk ($H \ll r$), unless r is close to $r_{\rm co}$ or $n \ll 1$.

In the case of molecular disks around YSOs, it is possible to estimate η directly from an explicit determination of the electron-molecule collision frequency for given temperature and density. Adopting the expressions given in Meyer & Meyer-Hofmeister (1999), we have $\eta = 10^{3.99} T_3^{1/2}(n_n/n_e)$, where T_3 is the temperature in units of 10^3 K, and where the electron–to–neutral number density ratio is calculated by assuming ionization equilibrium of alkali metals (primarily potassium) and is given by $\log(n_e/n_n) = 6.48 - 10.94/T_3 + 0.75 \log T_3 - 0.5 \log n_n$. As an illustration, we consider T Tauri stars, which are relatively slow rotators (mean rotation rate $\Omega_* \sim 10^{-5}$ s^{-1}), and for which we infer (assuming a 0.5 $M_\odot$ star) $r_{\rm co} \sim 10^{12}$ cm. D'Alessio et al. (1998) modeled accretion disks around such stars, and for a typical accretion rate of $10^{-8}\ M_\odot$ yr^{-1} and a disk "α parameter" of 0.01, we infer from their results values of $\sim 2 \times 10^3$ K and $\sim 7 \times 10^{15}$ cm^{-3} for the midplane temperature and particle density, respectively, at $r_{\rm co}$. For these values, we get $\eta \sim 7 \times 10^{10}$ cm s^{-2}, which is 5 orders of magnitude smaller than the nominal maximum turbulent diffusivity $c_{\rm s} H$. Although the estimated diffusivity increases at larger radii, we consider the region interior to $r_{\rm co}$ to be particularly relevant since the disk must extend to $r \le r_{\rm co}$ if matter is to be accreted onto the star. Note also that, as r increases above $r_{\rm co}$, $|\Delta\Omega| \to \Omega_*$ and $\Sigma_{\rm max}$ itself decreases with r ($\propto 1/r$). We conclude that result (4.7) is likely to represent a lower bound on the ratio $\Sigma/\Sigma_{\rm max}$ in many practical applications.

The preceding discussion indicates that it is unlikely that a disk with a dipole-like field configuration will achieve a steady state. It can, however, be seen from Table 1 that $h_{d,\,\rm max} \sim 1/n$ for $n \le 1$. (Note that BH96 demonstrate that $h_d \to 1/n$ as $n \to 0$.) Therefore, for sufficiently small n, $\Sigma_{\rm max}$ could be large enough for a steady state to be attainable even for realistic values of Σ. In § 4.2 we argue that if resistive diffusion in the radial (and not only azimuthal) direction is taken into account, then small effective values of n are also required for a steady state (in both the exact and time-averaged senses).

4.2. *Radial Flux Diffusion*

Since we include resistive diffusion in the azimuthal direction, for consistency we also need to consider *radial diffusion* and its effect on $B_{d,z}(r)$.

The radial speed of the magnetic field footpoints in their resistive diffusion across the disk can be written as $v_{{\rm B},r} = cE_{d,\phi}/B_{d,z} = cK_\phi/\Sigma B_{d,z}$, where $E_{d,\phi}$ is the azimuthal electric field and $K_\phi \approx 2Hj_\phi(z = 0)$ is the vertically integrated azi-

muthal current density. Setting $K_\phi = cB_{d,r}/2\pi$, where $B_{d,r} = B_r(r, \pi/2)$, one gets

$$v_{B,r}(r, t) = \frac{c^2}{2\pi\Sigma}\frac{B_{d,r}}{B_{d,z}} = \frac{c^2}{2\pi\Sigma} f[\pi/2, a_0(t)] . \quad (4.8)$$

(Note that if the effective conductivity is described by eq. [4.6], then $v_{B,r}(r, t) = \beta c_s f[\pi/2, a_0(t)]$; i.e., the footpoints move radially across the disk with roughly the sound speed, much faster than the radial gas velocity in a standard accretion disk!)

As we noted in § 2.3, $B_{d,r}/B_{d,z}$ diverges as $\Delta\Phi \to \Delta\Phi_c$. Indeed, in this limit, $a_0 \to 0$, and equations (2.4) and (2.19) then give $f(\pi/2) = g'(\pi/2)/n \to a_0^{-n} G_0'(\pi/2)/n$. But $G_0'(\pi/2)$ is finite and independent of a_0, so

$$v_{B,r} \propto f(\pi/2, a_0) \propto a_0^{-n} \to \infty , \quad \Delta\Phi \to \Delta\Phi_c . \quad (4.9)$$

Now, the conclusion about the finite-time singularity is based on the assumption that the field-line footpoints are fixed in the disk at all times. In reality, the footpoints would undergo some radial excursion Δr during the twisting time t_c from $\Delta\Phi = 0$ to $\Delta\Phi = \Delta\Phi_c$. If $\Delta r \ll r$, our results would not change much, but if $\Delta r/r \gtrsim 1$, then the approach to a singularity would need to be reexamined. In the high-conductivity limit ($\Sigma \gg c^2/\Delta\Omega r$ or $\eta \ll \Delta\Omega H r$) we can neglect the azimuthal resistive slippage and use equation (2.11) (especially near the critical point, where $B_{d,\phi} \to 0$). Assuming that $\Sigma = \text{const}$, the total radial footpoint displacement is

$$\Delta r = \frac{c^2}{2\pi\Sigma}\int_0^{t_c} f[\pi/2, a_0(t)]dt = \frac{c^2}{2\pi\Sigma\Delta\Omega}\int_{\Delta\Phi=0}^{\Delta\Phi_c}\left(\frac{d\Delta\Phi}{da_0}\right) f(\pi/2, a_0)da_0 . \quad (4.10)$$

Note that if $\Sigma \propto 1/r$, resistive slippage does not break the self-similarity assumption: $\Delta r \propto r$, and the self-similar scaling of the flux distribution $\Psi_d(r)$ (i.e., the power-law index n) remains unaffected by the footpoint migration.

Equation (4.9) describes the asymptotic behavior of $f(\pi/2)$ in the limit $\Delta\Phi \to \Delta\Phi_c$. The calculation of $(d\Delta\Phi/da_0)$ in this limit is more cumbersome and is given in the Appendix. Equation (A8) from the Appendix gives $\Delta\Phi \simeq \Delta\Phi_c + \xi a_0^n$, so that

$$\frac{d\Delta\Phi}{da_0} \propto a_0^{n-1} , \quad a_0 \to 0 . \quad (4.11)$$

Plugging equations (4.9) and (4.11) into equation (4.10), we obtain

$$\Delta r(\Delta\Phi \to \Delta\Phi_c) \sim \frac{c^2}{2\pi\Sigma\Delta\Omega}\int^{a_0\to 0} a_0^{-n} a_0^{n-1} da_0 \propto \log a_0 \to \infty , \quad a_0 \to 0 . \quad (4.12)$$

For example, in the case of turbulent diffusivity described by equation (4.6), we have

$$\Delta r \sim \frac{\beta c_s}{\Delta\Omega} |\log(\Delta\Phi_c - \Delta\Phi)| \to \infty , \quad \Delta\Phi \to \Delta\Phi_c . \quad (4.13)$$

This shows that, in principle, even if the conductivity is large, the radial field diffusivity in the disk cannot be neglected. As $\Delta\Phi \to \Delta\Phi_c$, the radial displacement Δr of the magnetic footpoints eventually becomes of order r, and the approximation $B_{d,z}(r) \approx \text{const}$ becomes inadequate. This outward migration would decrease $B_{d,r}$ and prevent it from blowing up. It can be argued, however, that the finite-time singularity would still occur. Indeed, as $t \to t_c$, Δr only scales logarithmically with a_0, but the radius $r(\Psi, \theta_{ap})$ of the apex point of the field line Ψ increases as a_0^{-1}. Thus, the twisted field lines expand much faster in the magnetosphere than their footpoints migrate inside the disk and so would still open in a finite time. Although inertial effects reduce the expansion speed in the magnetosphere (see Paper II), this speed would still be much higher than the field diffusion speed in the disk. In addition, because Δr diverges merely logarithmically as $\Delta\Phi \to \Delta\Phi_c$, the value of the twist angle at which Δr becomes of order r is *exponentially* close to $\Delta\Phi_c$. Taking, for example, the result (4.13) for the case of turbulent magnetic diffusivity, we get

$$\Delta\Phi_c - \Delta\Phi|_{\Delta r \sim r} \sim \exp\left[-\frac{Cr\Delta\Omega}{\beta c_s}\right] \ll 1 , \quad (4.14)$$

where $C \sim O(1)$. Thus, for any real system, the force-free equilibrium model ceases to be valid well before this point is reached.

The effect of the divergent radial field diffusion near $\Delta\Phi_c$ would be even less of an issue if reconnection in the magnetosphere terminated the expansion (e.g., Aly & Kuijpers 1990; VB94; Goodson et al. 1997, 1999). In this case, one may get periodic cycles of twisting, expansion, and reconnection Will the system maintain a *time-averaged* steady state in this case? VB94, who first addressed this question, noticed that, if $n < 1$, $B_{d,r}$ (and hence $v_{B,r}$) changes sign in the course of the evolution (see Fig. 2). Thus, depending on the twist angle at which reconnection occurs, there will be a value of $n \in (0,1)$ for which $B_{d,r}$ averages to zero between the start of the twisting cycle ($\Delta\Phi = 0$) and the point of reconnection.

An alternative scenario, also for $n < 1$, was proposed for an *exact* steady state by BH96 and later extended by Agapitou & Papaloizou (2000), who succeeded in calculating numerically true steady state equilibria (i.e., equilibria with $B_{d,r} = 0$ and with $B_{d,\phi}$ determined from the steady state condition [4.3]) for a Keplerian disk. We can gain further physical insight by reinterpreting both of these groups' conclusions in the language of the self-similar model as follows. The basic idea is that a system with $0 < n < 1$ attains $B_{d,r} = 0$ at some twist angle $\Delta\Phi_0 < \Delta\Phi_{max}$ (see Table 1). Then, if $\Delta\Phi_0$ *happens to be equal to* $\Delta\Phi_{ss}$, a genuine steady state with $B_{d,r} = 0$ (and with $B_{d,\phi} = B_{\phi,ss}$; see § 4.1) is established. However, since $\Delta\Phi_{ss}$ is directly related to Σ, this is possible only for some special $\Sigma = \Sigma_{ss}(n)$, which, in general, is unrealistically large (of order $c^2/r\Delta\Omega$; see § 4.1).

Both the VB94 and the BH96 proposals could probably be realized only when $n \ll 1$. In the VB94 scenario, this follows because one expects reconnection to occur only very close to $\Delta\Phi_c$, whereas in the BH96 scenario this is because, for realistic values of Σ, a steady state requires $h_{d,max} \gg 1$, and hence $n \ll 1$. In fact, one can interpret the conclusions of BH96 and Agapitou & Papaloizou (2000) in the language of the present paper as the argument that, for a given Σ, the radial field diffusion leads to a rearrangement of Ψ on the disk surface. This rearrangement has the effect of decreasing n to some small value $n = n_{ss}(\Sigma)$, such that $\Delta\Phi_{max}(\Sigma, n_{ss}) = \Delta\Phi_0(n_{ss})$. Whether this can happen in a real system depends, in particular, on the radial profile of Σ.

5. SUMMARY

In this paper we considered the time evolution of the magnetic field that threads an accretion disk around a magnetized star, resulting from the relative rotation between the disk and the star. We studied this evolution using simplified models of axisymmetric, force-free fields. In particular, we first employed the semianalytic self-similar solution first derived for a uniformly rotating disk by VB94 (see also Lynden-Bell & Boily 1994) to construct a sequence of magnetospheric equilibria parametrized by the relative twist angle $\Delta\Phi$. Subsequently, we tested the generality of our basic conclusions by constructing numerical solutions of the Grad-Shafranov equation for systems with rotation laws that approximate a Keplerian disk. Our main results and their astrophysical implications can be summarized as follows.

Assuming that both the star and the magnetosphere are perfectly conducting, the behavior of the twisted field lines depends on the surface conductivity Σ of the disk. A steady state configuration can be established only if, at a radius r in the disk, $\Sigma(r)$ is less than a certain limiting value, $\Sigma(r) < \Sigma_{\max}(r) \sim c^2/r|\Delta\Omega(r)|$ (see eq. [4.4]). In practice, $\Sigma_{\max}$ appears to be unrealistically small, and weakly ionized protostellar disks and even disks that possess a turbulent magnetic diffusivity typically do not satisfy the above condition, except very close to the corotation radius. Moreover, the inequality $\Sigma < \Sigma_{\max}$ is actually not sufficient for a steady state. In fact, $\Sigma(r)$ must be exactly equal to a certain specific value (which depends on the flux distribution profile at the surface of the disk) in order for the system to avoid radial flux diffusion (see § 4.2). Thus, we conclude that an exact steady state is very unlikely in magnetically linked star-disk systems.

Most astrophysical disks have $\Sigma(r) \gg \Sigma_{\max}(r)$ and are, therefore, not in a steady state. The field lines in these systems undergo secular twisting and, as a result, inflate and effectively open up when a critical twist angle $\Delta\Phi_c$ (on the order of a few rad) is reached. This finite-time singularity is an exact result of the self-similar model (VB94), but its presence in a general non–self-similar situation (e.g., a Keplerian disk) is supported by our numerically constructed sequences of two-dimensional force-free equilibria and by the simple physical argument given in § 3.

We also studied the effect of the radial field diffusion present in the case of a nonzero disk resistivity. We found that, as the field lines undergo a strong expansion, the increased radial magnetic field $B_{d,r}$ at the disk surface causes the field lines to migrate outward. A similar conclusion was also reached by Bardou & Heyvaerts (1996), who suggested, in addition, that the field lines would be expelled from the disk. We argued, however, that if one starts with a disk flux distribution $\Psi \propto r^{-n}$ with $n \sim O(1)$, then this expulsion is unlikely to happen on the rotation timescale. This is because the radial diffusion in the disk is much slower than the field-line expansion in the magnetosphere unless $n \ll 1$. Over many rotation periods, however, the radial diffusion could, in principle, lead to the establishment of a steady state via a drastic rearrangement of the flux, as discussed by BH96 and Agapitou & Papaloizou (2000).

Alternatively, a *time-averaged steady state* could, in principle, be attained in certain cases. In particular, this may happen if the field lines expand and reconnect in a cyclic manner and the cycle-averaged $B_{d,r}$ is zero (VB94), or if the cycle involves inward radial mass motions that counter the outward radial flux diffusion, as was evidently the case in the time-dependent numerical simulations of Goodson et al. (1999).

We thank Fred Lamb, B. C. Low, Oded Regev, Bob Rosner, and Aad van Ballegooijen for interesting and fruitful discussions. This research was supported in part by NASA grant NAG 5-1485 and the ASCI/Alliances Center for Astrophysical Thermonuclear Flashes at the University of Chicago under Department of Energy subcontract B341495 (D. U. and C. L.) and by NASA grant NAG 5-3689 (A. K.).

APPENDIX

CALCULATION OF $(d\Delta\Phi/da_0)$ NEAR THE CRITICAL POINT

In this appendix we analyze the behavior of the magnetic field near the critical point in more detail. Our main goal is to find the asymptotic behavior of $(d\Delta\Phi/da_0)$ near $\Delta\Phi_c$. We use the results of this analysis in § 4.2 to determine the effects of resistive diffusion near the critical point.

Calculating $(d\Delta\Phi/da_0)$ is not a straightforward task, since one needs to know the deviation of $g(\theta)$ from the asymptotic solution $G_0(\theta)a_0^{-n}$. Indeed, if one simply uses the lowest order expression $g(\theta) \simeq G_0(\theta)a_0^{-n}$ and plugs it into equation (2.12), one gets equation (2.20). Thus, in order to find the behavior of $(d\Delta\Phi/da_0)$ near $\Delta\Phi_c$, one needs to know the next-order (in a_0) correction to $g(\theta)$ as $a_0 \to 0$. Let us write

$$g(\theta) = G(\theta)a_0^{-n} = G_0(\theta)a_0^{-n} + \delta G(\theta)a_0^{-n}\,, \tag{A1}$$

where $G(\theta)$ is the solution of (2.18) satisfying $G(0) = 0$, $G(\pi/2) = a_0^n \ll 1$.

In order to find the correction $\delta G(\theta)$, let us introduce a small parameter ϵ chosen so that $\delta G(\pi/2 - \epsilon) \ll G_0(\pi/2 - \epsilon)$ and at the same time $\epsilon \ll 1$. As can be seen from Figure 3, the derivative $dG_0/d\theta$ at $\theta = \pi/2$ is finite (i.e., does not scale with a_0), and so $G_0(\pi/2 - \epsilon) \simeq \epsilon dG_0/d\theta(\pi/2)$. Next, $\delta G(\pi/2 - \epsilon) \sim \delta G(\pi/2) = a_0^n$, so we must choose ϵ in the range

$$a_0^n \ll \epsilon \ll 1\,. \tag{A2}$$

Inside the ϵ vicinity of $\theta = \pi/2$ we can approximate $\sin\theta \approx 1$, so we get

$$G''(\theta) + n(n+1)G + \frac{n}{n+1}\,G^{1+2/n} = 0\,. \tag{A3}$$

Since $G(\theta) \ll 1$ in this region, the solution can be written as

$$G_{\rm inner}(\theta) \simeq a_0^n + \text{const} \times (\theta - \pi/2) \, . \tag{A4}$$

In the region $\theta < \pi/2 - \epsilon$, $\delta G \ll G_0(\theta)$, and we can linearize equation (2.18), which gives

$$\sin(\theta) \frac{d}{d\theta}\left(\frac{1}{\sin\theta}\frac{d\delta G}{d\theta}\right) + n(n+1)\delta G(\theta) + \frac{n+2}{n+1}\,\delta G(\theta)[G_0(\theta)]^{2/n} = 0 \, . \tag{A5}$$

Actually, near $\theta = \pi/2$ the last term of equation (A5) becomes negligible compared with the other terms (because $G_0(\theta) \ll 1$ there). Since this is the only term that distinguishes this equation from the one describing the inner region $\theta > \pi/2 - \epsilon$, we can ignore the difference and extend the range of applicability of equation (A5) all the way up to $\theta = \pi/2$, where we set the boundary condition $\delta G(\pi/2) = a_0^n$. The other boundary condition is $\delta G(0) = 0$.

Once $\delta G(\theta)$ is known, one can determine the asymptotic behavior of $\Delta\Phi(a_0)$ as $a_0 \to 0$. We write $\Delta\Phi = \Delta\Phi_c + \delta\Delta\Phi$, where

$$\delta\Delta\Phi = \frac{1}{n+1}\int_0^{\pi/2} \delta[G^{1/n}(\theta)]\,\frac{d\theta}{\sin\theta} \, . \tag{A6}$$

In order to estimate this integral, let us choose some $\epsilon_1 \sim a_0^{n-x} \ll 1$, $0 < x < n$. Then, within the ϵ_1-vicinity of $\theta = \pi/2$, we have $G(\theta) \simeq a_0^n + G_0(\theta)$ and $G_0(\theta) \simeq [dG_0/d\theta]|_{\theta=\pi/2}(\theta - \pi/2) \sim C_1\epsilon_1$. Hence $|\delta[G^{1/n}(\theta)]| < C_2\epsilon_1^{1/n}$ in this region, where C_1, $C_2 = O(1)$, and we can estimate this region's contribution to the integral (A6) as

$$\left|\frac{1}{n+1}\int_{\pi/2-\epsilon_1}^{\pi/2} \delta[G^{1/n}(\theta)]\,\frac{d\theta}{\sin\theta}\right| < C_3\epsilon_1^{1+1/n} \, , \qquad C_3 = O(1) \, . \tag{A7a}$$

In the rest of the integration domain, $\delta[G^{1/n}(\theta)] \simeq (1/n)(\delta G)G_0^{1/n-1}(\theta)$, and so

$$\frac{1}{n+1}\int_0^{\pi/2-\epsilon_1} \delta[G^{1/n}(\theta)]\,\frac{d\theta}{\sin\theta} \simeq \frac{1}{n+1}\int_0^{\pi/2-\epsilon_1} \frac{\delta G}{n}\,G_0^{1/n-1}(\theta)\,\frac{d\theta}{\sin\theta} \, . \tag{A7b}$$

Since $\delta G \sim a_0^n$, the contribution from this region is of order a_0^n. Thus, if we choose ϵ_1 so that $\epsilon_1^{1+1/n} \ll a_0^n$, and hence $x < n/(n+1)$, then this contribution will be much larger than the contribution from the ϵ_1-vicinity of $\theta = \pi/2$. Thus, the correction to $\Delta\Phi$ is on the order of a_0^n, and we now calculate the coefficient. Notice that the integral (A7b) as a function of ϵ_1 converges in the limit $\epsilon_1 \to 0$. Therefore, to lowest order in a_0, we can write

$$\delta\Delta\Phi \simeq \frac{1}{n(n+1)}\int_0^{\pi/2} \delta G G_0^{1/n-1}(\theta)\,\frac{d\theta}{\sin\theta} = \xi(n)a_0^n \, . \tag{A8}$$

Using the functions δG and $G_0(\theta)$ obtained above, we get, for example, $\delta\Delta\Phi(n=1) \approx -0.17a_0$ and $\delta\Delta\Phi(n=0.5) \approx -0.22a_0^{1/2}$ as $a_0 \to 0$.

REFERENCES

Agapitou, V., & Papaloizou, J. C. B. 2000, MNRAS, 317, 273
Aly, J. J. 1984, ApJ, 283, 349
———. 1985, A&A, 143, 19
———. 1995, ApJ, 439, L63
Aly, J. J., & Kuijpers, J. 1990, A&A, 227, 473
Amari, T., Luciani, J. F., Aly, J. J., & Tagger, M. 1996a, A&A, 306, 913
———. 1996b, ApJ, 466, L39
Bardou, A., & Heyvaerts, J. 1996, A&A, 307, 1009 (BH96)
Barnes, C. W., & Sturrock, P. A. 1972, ApJ, 174, 659
Bertout, C., Basri, G., & Bouvier, J. 1988, ApJ, 330, 350
Bertout, C., Harder, S., Malbet, F., Mennessier, C., & Regev, O. 1996, AJ, 112, 2159
Bouvier, J., Carbit, S., Fernandez, M., Martin, E. L., & Matthews, J. M. 1993, A&A, 272, 176
Campbell, C. G. 1992, Geophys. Astrophys. Fluid Dyn., 63, 179
Collier Cameron, A., & Campbell, C. G. 1993, A&A, 274, 309
Collier Cameron, A., Campbell, C. G., & Quaintrell, H. 1995, A&A, 298, 133
D'Alessio, P., Cantó, J., Calvet, N., & Lizano, S. 1998, ApJ, 500, 411
Daumerie, P. R. 1996, Ph.D. thesis, Univ. Illinois, Urbana-Champaign
Edwards, S., Hartigan, P., Ghandour, L., & Andrulis, C. 1994, AJ, 108, 1056
Edwards, S., et al. 1993, AJ, 106, 372
Ghosh, P. 1995, MNRAS, 272, 763
Ghosh, P., & Lamb, F. K. 1978, ApJ, 223, L83
———. 1979a, ApJ, 232, 259
———. 1979b, ApJ, 234, 296
Goodson, A. P., Böhm, K.-H., & Winglee, R. M. 1999, ApJ, 524, 142
Goodson, A. P., & Winglee, R. M. 1999, ApJ, 524, 159
Goodson, A. P., Winglee, R. M., & Böhm, K.-H. 1997, ApJ, 489, 199
Hartmann, L. 1997, in Herbig-Haro Flows and the Birth of Low Mass Stars, ed. B. Reipurth & C. Bertout (Dordrecht: Kluwer), 391
Hartmann, L., Hewett, R., & Calvet, N. 1994, ApJ, 426, 669
Hayashi, M. R., Shibata, K., & Matsumoto, R. 1996, ApJ, 468, L37
Herbst, W., Rhode, K. L., Hillenbrand, L. A., & Curran, G. 2000, AJ, 119, 261
Johns-Krull, C. M., & Basri, G. 1997, ApJ, 474, 433
Johns-Krull, C. M., & Hatzes, A. P. 1997, ApJ, 487, 896
Klimchuk, J. A., & Sturrock, P. A. 1989, ApJ, 345, 1034
Königl, A. 1991, ApJ, 370, L39
Lamb, F. K. 1989, in Timing Neutron Stars, ed. H. Ögelman & E. P. J. van den Heuvel (Dordrecht: Kluwer), 649
Lamzin, S. A. 1995, A&A, 295, L20
Lovelace, R. V. E., Romanova, M. M., & Bisnovatyi-Kogan, G. S. 1995, MNRAS, 275, 244 (LRBK95)
Low, B. C. 1986, ApJ, 307, 205
Low, B. C., & Lou, Y. Q. 1990, ApJ, 352, 343
Lynden-Bell, D., & Boily, C. 1994, MNRAS, 267, 146
Martin, E. L. 1997, A&A, 321, 492
Meyer, F., & Meyer-Hofmeister, E. 1999, A&A, 341, L23
Mikić, Z., & Linker, J. A. 1994, ApJ, 430, 898
Miller, K. A., & Stone, J. M. 1997, ApJ, 489, 890
Muzerolle, J., Hartmann, L., & Calvet, N. 1998, AJ, 116, 455
Parker, E. N. 1979, Cosmical Magnetic Fields (Oxford: Oxford Univ. Press)
Patterson, J. 1994, PASP, 106, 209
Roumeliotis, G., Sturrock, P. A., & Antiochos, S. K. 1994, ApJ, 423, 847
Safier, P. N. 1998, ApJ, 494, 336
Shakura, N. I., & Sunyaev, R. A. 1973, A&A, 24, 337
Uzdensky, D. A., Königl, A., & Litwin, C. 2002, ApJ, 565, 1205 (Paper II)
van Ballegooijen, A. A. 1994, Space Sci. Rev., 68, 299 (VB94)
Wang, Y.-M. 1987, A&A, 183, 257
Wolfson, R. 1995, ApJ, 443, 810
Wolfson, R., & Low, B. C. 1992, ApJ, 391, 353
Yi, I. 1994, ApJ, 428, 760
———. 1995, ApJ, 442, 768
Yi, I., Wheeler, J. C., & Vishniac, E. T. 1997, ApJ, 491, L93
Zylstra, G. J. 1988, Ph.D. thesis, Univ. Illinois, Urbana-Champaign